

Cosmological Parameters and Cosmic Topology

M.J. Rebouças¹* and J. S. Alcaniz²†

¹Centro Brasileiro de Pesquisas Físicas, Rua Dr. Xavier Sigaud 150, 22290-180 Rio de Janeiro – RJ, Brazil
²Observatório Nacional, Rua Gal. José Cristino 77, 20921-400, São Cristóvão, Rio de Janeiro - RJ, Brazil

Accepted ; Received

ABSTRACT

Geometry constrains but does not dictate the topology of the 3-dimensional space. In a locally spatially homogeneous and isotropic universe, however, the topology of its spatial section dictates its geometry. We show that, besides determining the geometry, the knowledge of the spatial topology through the circles-in-the-sky offers an effective way of setting constraints on the density parameters associated with dark matter (Ω_m) and dark energy (Ω_Λ). By assuming the Poincaré dodecahedral space as the circles-in-the-sky detectable topology of the spatial sections of the Universe, we re-analyze the constraints on the density parametric plane $\Omega_m - \Omega_\Lambda$ from the current type Ia supernovae (SNe Ia) plus X-ray gas mass fraction data, and show that a circles-in-the-sky detection of the dodecahedral space topology give rise to strong and complementary constraints on the region of the density parameter plane currently allowed by these observational data sets.

Key words: Cosmology: theory - dark matter - distance scale

1 INTRODUCTION

The standard approach to cosmological modelling commences with the assumption that our 3-dimensional space is homogeneous and isotropic at large scales. The most general spacetime metric consistent with the existence of a cosmic time t and the principle of spatial homogeneity and isotropy is

$$ds^2 = -dt^2 + a^2(t) [dx^2 + f^2(\chi)(d\theta^2 + \sin^2 \theta d\phi^2)] , \quad (1)$$

where $f(\chi) = (\chi, \sin \chi, \sinh \chi)$ depending on the sign of the constant spatial curvature ($k = 0, 1, -1$), and $a(t)$ is the cosmological scale factor. The metric (1) only express the above assumptions, it does not specify the underlying spacetime manifold \mathcal{M}_4 nor the corresponding spatial sections M . In this geometrical approach to model the physical world the dynamics of the Universe is clearly provided by a metrical theory of gravitation as, for example, General Relativity.

The Friedmann equation $k = H_0^2 a_0^2 (\Omega_{\text{tot}} - 1)$ ¹ makes apparent that the curvature (or the corresponding geometry) of the spatial section M of the Universe is an observable in that for $\Omega_{\text{tot}} > 1$ the spatial section is positively curved, for $\Omega_{\text{tot}} = 1$ it is flat ($k = 0$), while for $\Omega_{\text{tot}} < 1$ it is nega-

tively curved. Thus, a chief point in the search for the (spatial) geometry of universe is to constrain the density Ω_{tot} from observations. In the context of the current standard cosmological model, i.e., the Λ CDM scenario, this amounts to determining regions in the density parametric plane $\Omega_m - \Omega_\Lambda$, which consistently account for the observations, and from which one expects to infer the spatial geometry of the Universe.

In practice, to observationally probe the spatial geometry of the Universe, by using, e.g., a single observational data set as the current type Ia supernovae (SNe Ia) observations, various degeneracies arise in the parametric plane $\Omega_m - \Omega_\Lambda$ (Riess et al. 2004). These degeneracies are mitigated by either imposing reasonable priors, or combining the data with complementary observations, or both. An example in this regard is the combination of the current Supernovae Ia (SNIa) compilation (Riess et al. 2004) with the Sloan Digital Sky Survey (SDSS) galaxy power spectrum (Tegmark et al. 2004) and the cosmic microwave background (CMB) measurements by the Wilkinson Microwave Anisotropy Probe [WMAP] (Bennet et al. 2003; Spergel et al. 2003), which has remarkably narrowed the bounds on the cosmological density parameters Ω_m and Ω_Λ . Besides being sensitive to different combination of the density parameters, these measurements probe the geometry of the Universe at considerably different redshifts (typically $z < 2$ for SNe Ia or $z \sim 1100$ for CMB).

However, the spatial geometry constrains but does not dictate the topology of the 3-space M , and although the spatial section M is usually taken to be one of the simply-

* E-mail: reboucas@cbpf.br

† E-mail: alcaniz@on.br

¹ The total density at the present time t_0 is $\Omega_{\text{tot}} = \rho_{\text{tot}}/\rho_{\text{crit}}$ with $\rho_{\text{crit}} \equiv 3H_0^2/8\pi G$, and a_0 and H_0 are, respectively, the scale factor and the Hubble parameter at t_0 .

2 Rebouças and Alcaniz

connected spaces, namely Euclidean \mathcal{R}^3 , spherical \mathcal{S}^3 , or hyperbolic \mathcal{H}^3 , it is a mathematical result that great majority of locally homogeneous and isotropic 3–spaces M are multiply-connected quotient manifolds of the form \mathcal{R}^3/Γ , \mathcal{S}^3/Γ , and \mathcal{H}^3/Γ , where Γ is a fixed-point free group of isometries of the corresponding covering space. Thus, for example, for the Euclidean geometry ($k = 0$) besides \mathcal{R}^3 there are 6 classes of topologically distinct compact orientable spaces M that can be endowed with this geometry, while for both the spherical ($k = 1$) and hyperbolic ($k = -1$) geometries there are an infinite number of topologically inequivalent manifolds with non-trivial topology that can be endowed with each one of these geometries.

Now since the spatial geometry is an observable that constrains but does not determine the topology of the 3–space M , two pertinent questions at this point are whether the topology may be an observable and, if so, to what extent it can be used to remove or at least reduce the degeneracies in the density parameter plane $\Omega_m - \Omega_\Lambda$, which arise from statistical analyses with data from current observations.

The main aim of this paper, which extends and complements our previous work (Rebouças et al. 2005), is to address these questions in the context of the Λ CDM scenario, by focusing our attention on the finite and positively curved Poincaré space model (Luminet et al. 2003) that accounts for the suppression of power at large scales observed by WMAP(Bennet et al. 2003; Spergel et al. 2003), and also fits the WMAP temperature two-point correlation function (Aurich et al. 2005a; 2005b; Gudermann 2005). In other words, we shall show how to use the Poincaré dodecahedral space as a circles-in-the-sky observable topology of the Universe² to reduce the inherent degeneracies in the density parameters Ω_m and Ω_Λ that arise from the so-called *gold* set of 157 SNe Ia, as compiled by Riess et al. (2004), along with the latest Chandra measurements of the X-ray gas mass fraction in 26 galaxy clusters, as provided by Allen et al. (2004).

2 COSMIC TOPOLOGY

In a number of recent papers different strategies and methods to probe a non-trivial topology of the spatial section of the Universe have been discussed (see, e.g., Lehoczky et al, 1996; Roukema and Edge, 1997; Gomero et al., 2002; Fagundes and Gausmann, 1999; Uzan et al, 1999; Hajian and Souradeep, 2005; Hajian et al., 2005; and the review articles Lachièze-Rey and Luminet, 1995; Starkman, 1998; Levin, 2002; Rebouças and Gomero, 2004). An immediate observational consequence of a detectable non-trivial topology³ of the 3–space M is that the sky will show multiple (topological) images of either cosmic objects or repeated patterns of the cosmic microwave background radiation (CMBR). Here, we shall focus on the so-called “circles-in-the-sky” method,⁴

² Here, in line with the usage in the literature, by topology of the universe we mean the topology of the space-like section M .

³ For a detailed discussion on the extent to which a non-trivial topology may or may not be detected see Gomero et al. 2001a; 2001b; Weeks et al., 2003; Weeks, 2003.

⁴ For details on the other CMB ‘approaches to cosmic topology’ see, e.g., Levin et al., 1998; Bond et al., 2000; Hajian and T.

which relies on multiple copies of correlated circles in the CMBR maps (Cornish et al. 1998), whose existence is clear from the following reasoning: in a universe with a detectable non-trivial topology, the sphere of last scattering necessarily intersects some of its topological images along pairs of circles of equal radii, centered at different points on the last scattering sphere (LSS), with the same distribution of temperature fluctuations, δT , along the circles correlated by an element g of the covering group Γ . Since the mapping from the last scattering surface to the night sky sphere preserves circles (Penrose, 1959; Calvão et al., 2005), these pairs of matching circles will be written on the CMBR anisotropy sky maps regardless of the background geometry and for any non-trivial detectable topology. As a consequence, to observationally probe a non-trivial topology on the available largest scale, one should suitably scrutinize the full-sky CMB maps in order to extract the correlated circles, whose angular radii and relative position of their centers can be used to determine the topology of the universe. Thus, a non-trivial topology of the space section of the universe may be an observable, which can be probed through the circles in the sky for all locally homogeneous and isotropic universes with no assumption on the cosmological density parameters.

Regarding the question as to whether the topology can be used as an observable to reduce degeneracies in the cosmological density parameters, we first note that the topology of a locally homogeneous and isotropic 3–manifold determines the sign of its curvature (see, e.g., Bernshtein and Shvartsman, 1980), and therefore the topology of the spatial section M of the Universe dictates its geometry. As a consequence, the detection of a *generic* cosmic topology alone would give rise to a strong degeneracy on both density parameters, since it only determines whether the density parameters take values in the regions below, above, or on the flat line $\Omega_{\text{tot}} = \Omega_m + \Omega_\Lambda = 1$.

In what follows we examine to what extent a combination of the circles-in-the-sky detection of a *specific* spatial topology, namely, the Poincaré dodecahedral space topology (which accounts for some observed anomalies in WMAP CMB data) with the current SNIa and galaxy clusters measurements may reduce the intrinsic density parameter degeneracies of the $\Omega_m - \Omega_\Lambda$ plane.

2.1 Poincaré Dodecahedral Space Model

The Poincaré dodecahedral space \mathcal{D} is a manifold of the form \mathcal{S}^3/Γ in which $\Gamma = I^*$ is the binary icosahedral group of order 120. It is represented by a regular spherical dodecahedron (12 pentagonal faces) along with the identification of the opposite faces after a twist of 36° . Such a space is positively curved, and tiles the 3–sphere \mathcal{S}^3 into 120 identical spherical dodecahedra.

By assuming some priors and combining CMB data with other astronomical data, the WMAP team reported (Spergel et al. 2003) both the best fit value $\Omega_{\text{tot}} = 1.02 \pm 0.02$ (1σ level), which includes a positively curved universe as a realistic possibility, and account for the suppression of

Souradeep, 2003; Oliveira-Costa et al. 1996; 2004; Dineen et al. 2004; Donoghue and Donoghue, 2004; Copi et al. 2003; Hipolito-Ricaldi and Gomero, 2005.

power at wide angles ($\ell = 2$ and $\ell = 3$). These facts have motivated the suggestion by Luminet *et al.* (2003) of the Poincaré dodecahedral space topology as an explanation for the apparent discrepancy between the Λ CDM concordance model and WMAP data. Since then, the dodecahedral space has been examined in some works (Cornish *et al.*, 2004; Roukema *et al.*, 2004; Aurich *et al.*, 2005a; 2005b; Gudermann, 2005), in which some further features of the model have been carefully considered. As a result, it turns out that a universe with the Poincaré dodecahedral space section accounts for the suppression of power at large scales observed by WMAP, and fits the WMAP temperature two-point correlation function for $1.015 \leq \Omega_{\text{tot}} \leq 1.020$ (Aurich *et al.*, 2005a; 2005b), retaining the standard Friedmann–Lemaître–Robertson–Walker (FLRW) foundation for local physics.⁵ On this observational grounds, in what follows, we assume the Poincaré dodecahedron as the specific circles-in-the-sky detected 3-space topology of the Universe.

3 OBSERVATIONS

3.1 Method

An important class of manifolds with a non-trivial topology is comprised by the globally homogeneous manifolds. These manifolds satisfy a topological principle of (global) homogeneity, in the sense that all points in M are topologically equivalent. In particular, in these spaces the pairs of matching circles of the circles-in-the-sky method will be antipodal, as shown in Figure 1.

The Poincaré dodecahedral space (PDS) \mathcal{D} is globally homogeneous, and gives rise to six pairs of antipodal matched circles on the LSS, centered in a symmetrical pattern as the centers of the faces of the dodecahedron. Figure 1 gives an illustration of two of these antipodal circles. Clearly the distance between the centers of each pair of circles is twice the radius r_{inj} of the sphere inscribable in \mathcal{D} . Now, a straightforward use of a Napier's rule to the right-angled spherical triangle shown in Fig. 1 furnishes a relation between the angular radius α and the angular sides r_{inj} and radius χ_{lss} of the last scattering sphere, namely

$$\chi_{\text{lss}} = \tan^{-1} \left[\frac{\tan r_{\text{inj}}}{\cos \alpha} \right], \quad (2)$$

where r_{inj} is a topological invariant, equal to $\pi/10$ for the dodecahedral topology, and the distance χ_{lss} to the origin *in units of the curvature radius*, $a_0 = a(t_0) = (H_0 \sqrt{|1 - \Omega_{\text{tot}}|})^{-1}$, is given by

⁵ A preliminary search failed to find the antipodal and nearly antipodal matched circles with radii larger than 25° . This absence of evidence of correlated may be due to several causes, among which it is worth mentioning that Doppler and integrated Sachs–Wolfe contributions to these circles may be strong enough to blur them, and so the correlated circles can have been overlooked in the CMB maps search (Aurich *et al.*, 2005a). In this way, the ‘absence of evidence may not be evidence of absence’, specially given that effects such as Sunyaev–Zeldovich and the finite thickness of the LSS, as well as possible systematics in the removal of the foregrounds, can further damage the topological circle matching.

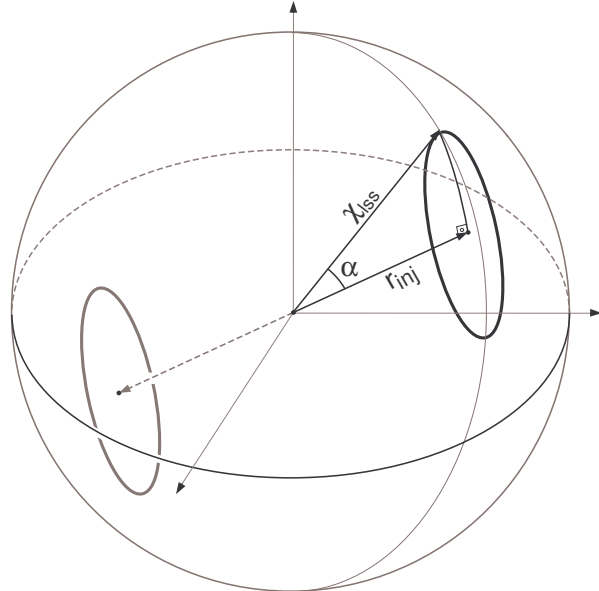


Figure 1. A schematic illustration of two antipodal matching circles in the sphere of last scattering. These pair of circles come about in all globally homogeneous positively curved manifolds with a detectable topology through the circles-in-the-sky method. The relation between the angular radius α and the angular sides r_{inj} and χ_{lss} is given by the following Napier's rule for spherical triangles: $\cos \alpha = \tan r_{\text{inj}} \cot \chi_{\text{lss}}$

$$\chi_{\text{lss}} = \frac{d_{\text{lss}}}{a_0} = \sqrt{|\Omega_k|} \int_1^{1+z} \frac{dx}{\sqrt{x^3 \Omega_m + x^2 \Omega_k + \Omega_\Lambda}}, \quad (3)$$

where d_{lss} is the radius of the LSS, $x = 1+z$ is an integration variable, $\Omega_k = 1 - \Omega_{\text{tot}}$, and $z_{\text{lss}} = 1089$ (Spergel *et al.* 2003).

Equations (2) and (3) give the relations between the angular radius α and the cosmological density parameters Ω_Λ and Ω_m , and thus can be used to set bounds on these parameters. To quantify this we proceed in the following way. Firstly, we assume the angular radius $\alpha = 50^\circ$, as estimated by Aurich *et al.* (2005a). Secondly, since the measurements of the radius α unavoidably involve observational uncertainties we take, in order to obtain very conservative results, $\delta\alpha \simeq 6^\circ$, which is the scale below which the circles are blurred (Aurich *et al.* 2005a).

3.2 Statistical Analysis

In order to study the effect of the PDS topology on the parametric space $\Omega_m - \Omega_\Lambda$, we use the most recent compilation of SNe Ia data, the so-called *gold* sample of 157 SNe Ia, recently published by Riess *et al.* (2004) along with the latest Chandra measurements of the X-ray gas mass fraction in 26 X-ray luminous, dynamically relaxed galaxy clusters spanning the redshift range $0.07 < z < 0.9$, as provided by Allen *et al.* (2004). We emphasize that this particular combination of observational data covers complementary aspects of the $\Omega_m - \Omega_\Lambda$ plane, in that while X-ray measurements are very effective to place limits on the clustered matter (Ω_m) the new SNe Ia sample tightly constrains the unclustered component (Ω_Λ).

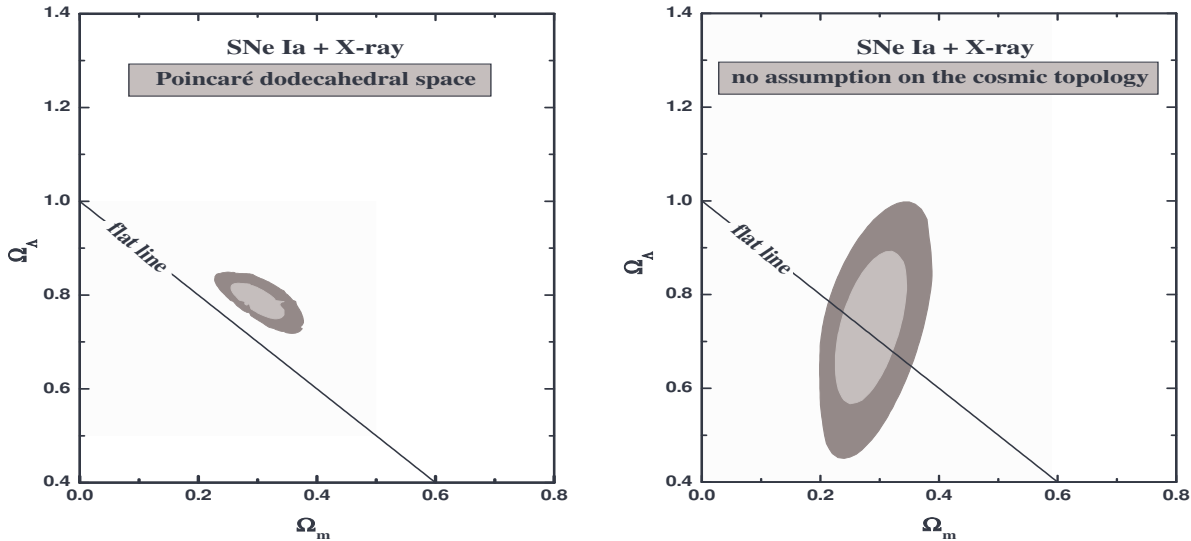


Figure 2. The results of our statistical analyses. The panels show confidence regions (68.3% and 95.4% c.l.) in the $\Omega_m - \Omega_\Lambda$ plane from the latest Chandra measurements of the X-ray gas mass fraction in 26 galaxy clusters ($0.07 < z < 0.9$) plus determinations of the baryon density parameter, measurements of the Hubble parameter and the *gold* sample of 157 SNe Ia. In the left panel a specific circles-in-the-sky detection of the dodecahedral space topology with $\alpha = 50^\circ$, $\delta\alpha = 6^\circ$ is assumed. The best fit values for the matter and vacuum density parameters are, respectively, $\Omega_m = 0.30 \pm 0.04$ and $\Omega_\Lambda = 0.79 \pm 0.03$ at 95.4% c.l., which provides $\Omega_{\text{tot}} \simeq 1.09 \pm 0.05$. In the right panel the conventional SNe Ia plus X-ray analysis is shown for comparison.

3.3 f_{gas} versus redshift test

The X-ray gas mass fraction test [$f_{\text{gas}}(z)$] was first introduced by Sasaki (1996) and further developed by Allen *et al.* (2002a; 2002b) (see also Ettori *et al.* 2003; Lima *et al.* 2003; 2004; Chen and Ratra 2004; Zhu and Alcaniz 2005; Alcaniz and Zhu 2005). This is based on the assumption that rich clusters of galaxies are large enough to provide a fair representation of the baryonic and dark matter distributions in the Universe (Fukugita *et al.* 1998). Following this assumption, the matter content of the Universe can be expressed as the ratio between the baryonic content and the gas mass fraction, i.e., $\Omega_m \propto \Omega_b/f_{\text{gas}}$. Moreover, as shown by Sasaki 1996, since $f_{\text{gas}} \propto d_A^{3/2}$ the model function can be defined as (Allen *et al.* 2002a)

$$f_{\text{gas}}^{\text{mod}}(z) = \frac{b\Omega_b}{(1 + 0.19\sqrt{h})\Omega_m} \left[2h \frac{d_A^{\text{E-dS}}(z)}{d_A^{\Lambda\text{CDM}}(z)} \right]^{1.5}, \quad (4)$$

where the bias factor b is a parameter motivated by gas dynamical simulations that takes into account the fact that the baryon fraction in clusters is slightly depressed with respect to the Universe as a whole (Eke *et al.* 1998; Bialek *et al.* 2003), the term $0.19\sqrt{h}$ stands for the optically luminous galaxy mass in the cluster and the ratio between the angular diameter distances $d_A^{\text{E-dS}}(z_i)/d_A^{\Lambda\text{CDM}}(z_i)$ accounts for deviations in the geometry of the Universe (here modelled by the ΛCDM model) from the default cosmology used in the observations, i.e., the Einstein-de Sitter (E-dS) model (see Allen *et al.* (2004) for more observational details).

In order to perform the f_{gas} test, three Gaussian priors are added to our analysis, namely, on the baryon density

parameter, $\Omega_b h^2 = 0.0224 \pm 0.0009$ (Spergel *et al.* 2003), on the Hubble parameter, $h = 0.72 \pm 0.08$ Freedman *et al.* (2001), and on the bias factor, $b = 0.824 \pm 0.089$ (Eke *et al.* 1998; Bialek *et al.* 2003). Thus, the total minimization $\chi^2_{f_{\text{gas}}}$ is written as

$$\chi^2_{f_{\text{gas}}} = \sum_{i=1}^{26} \frac{[f_{\text{gas}}^{\text{mod}}(z_i) - f_{\text{gas},i}]^2}{\sigma_{f_{\text{gas},i}}^2} + \left[\frac{\Omega_b h^2 - 0.0224}{0.0009} \right]^2 + \left[\frac{h - 0.72}{0.08} \right]^2 + \left[\frac{b - 0.824}{0.089} \right]^2, \quad (5)$$

where $f_{\text{gas}}^{\text{mod}}(z_i)$ is given by Eq. (4) and $f_{\text{gas},i}$ is the observed values of the X-ray gas mass fraction with errors $\sigma_{f_{\text{gas},i}}$.

3.4 Magnitude versus redshift test

Supernovae observations provide the most direct evidence for the current cosmic acceleration. To perform a statistical analysis with the current supernovae data we first define the predicted distance modulus for a supernova at redshift z , given a set of parameters \mathbf{s} , i.e.,

$$\mu_p(z|\mathbf{s}) = m - M = 5\log d_L + 25, \quad (6)$$

where m and M are, respectively, the apparent and absolute magnitudes, the complete set of parameters is $\mathbf{s} \equiv (h, \Omega_m, \Omega_\Lambda)$ and d_L stands for the luminosity distance (in units of megaparsecs).

The set of parameters \mathbf{s} is estimated by using a χ^2 statistics, with

$$\chi^2_{\text{SNe}} = \sum_{i=1}^{157} \frac{[\mu_p^i(z|\mathbf{s}) - \mu_o^i(z|\mathbf{s})]^2}{\sigma_i^2}, \quad (7)$$

where $\mu_p^i(z|\mathbf{s})$ is given by Eq. (6), $\mu_o^i(z|\mathbf{s})$ is the extinction corrected distance modulus for a given SNe Ia at z_i , and σ_i is the uncertainty in the individual distance moduli, which includes uncertainties in galaxy redshift due to a peculiar velocity of 400 km/s (For more details on statistical analyses involving SNe Ia observations we refer the reader to Padmanabhan and Choudhury, 2003; Zhu and Fujimoto, 2003; Nesseris and Perivolaropoulos, 2004; Alcaniz, 2004; Alcaniz and Pires, 2004; Choudhury and Padmanabhan, 2005; Shafieloo et al., 2005).

3.5 Topological constraint

Similarly to the Gaussian priors added to the f_{gas} test, the Poincaré dodecahedral space topology is included in our statistical analysis as a prior relative to the value of χ_{lss} , which can be easily obtained from a elementary combination of Eqs. (2) – (3). In other words, the contribution of the topology to our statistical analysis is a term of the form

$$\chi_{\text{topology}}^2 = \frac{(\chi_{lss}^{\text{Th}} - \chi_{lss}^{\text{Obs}})^2}{(\delta\chi_{lss})^2}, \quad (8)$$

where χ_{lss}^{Th} is given by Eq. (2) and the uncertainty $\delta\chi_{lss}$ comes from the uncertainty $\delta\alpha$ of the circles-in-the-sky. This means that the total χ_{total}^2 minimization function is given by

$$\chi_{\text{total}}^2 = \chi_{f_{\text{gas}}}^2 + \chi_{SNe}^2 + \chi_{\text{topology}}^2. \quad (9)$$

4 RESULTS AND DISCUSSIONS

The left panel in Figure 2 shows the results of our statistical analysis. Confidence regions – 68.3% and 95.4% confidence limits (c.l.) – in the parametric space $\Omega_m - \Omega_\Lambda$ are displayed for the particular combination of observational data described above. For the sake of comparison, we also show in the right panel the $\Omega_m - \Omega_\Lambda$ plane for the conventional SNe Ia plus Galaxy Clusters analaysis, i.e., the one without the above cosmic topology assumption. By comparing both analyses, it is clear that our initial premiss that a circles-in-the-sky detection of a non-trivial space topology reduces considerably the parametric space region allowed by the current observational data, and also breaks some degeneracies arising from the current SNe Ia and X-ray gas mass fraction measurements. The best-fit parameters for this SNe Ia+X-ray+Topology analysis are $\Omega_m = 0.30$ and $\Omega_\Lambda = 0.79$ with the reduced $\chi_\nu^2 \equiv \chi_{\text{min}}^2/\nu \simeq 1.12$ (ν is defined as degree of freedom). Note that such a value of χ_ν^2 is slightly smaller than the one obtained by fitting the *gold* sample of SNe Ia to the flat Λ CDM (concordance) scenario, i.e., $\chi_\nu^2 \simeq 1.14$, and equal to the value found for the Λ CDM model with arbitrary curvature (Riess et al, 2004). At 95.4% c.l. we also obtain $0.26 \leq \Omega_m \leq 0.34$ and $0.76 \leq \Omega_\Lambda \leq 0.82$ providing $\Omega_{\text{tot}} \simeq 1.09 \pm 0.05$, which is consistent at 2σ level with the value reported by the WMAP team, i.e., $\Omega_{\text{tot}} = 1.02 \pm 0.02$ at 1σ (Spergel et al 2003). Note also that the above best-fit scenario is in full agreement with most of the current observational analyses (see, e.g., Roos (2005) for an updated review) and corresponds to a current accelerated universe with $q_0 \simeq -0.64$ and a total expanding age of $9.67h^{-1}$ Gyr. Finally, we also emphasize that the best-fit values for both

Ω_m and Ω_Λ (and, consequently, for Ω_{tot}) does not depend very strongly on the value used for angular radius α , which means that the uncertainties on this parameter alter predominantly the area corresponding to the confidence regions, without having a very significant effect on the best-fit values, as well as on the complementary results of our statistical analysis. As an example, note – from Eq.(2) – that values of the angular radius lying in the range $0^\circ \leq \alpha \leq 90^\circ$ imply the following intervals for the cosmological density parameters: $0.32 \leq \Omega_m \leq 0.38$ and $0.7 \leq \Omega_\Lambda \leq 0.9$ or, equivalently, $1.02 \leq \Omega_{\text{tot}} \leq 1.28$.

5 CONCLUDING REMARKS

By assuming the Poincaré dodecahedral space as circles-in-the-sky detected topology of the spatial sections of the Universe, we have re-analyzed the constraints on the parametric space $\Omega_m - \Omega_\Lambda$ from the current SNe Ia and X-ray gas mass fraction data. As the main outcome of this analysis, we have shown that once detected the PDS topology along with the corresponding circles-in-the-sky, they give rise to very strong and complementary constraints on the region of density parameter plane currently allowed by the cosmological observations. We have also discussed how the degeneracies inherent to a joint analysis involving SNe Ia observations and X-ray gas mass fraction measurements are drastically reduced by the assumption of a circles-in-the-sky detection of a PDS topology. Finally, our results also indicate that cosmic topology may offer a fruitful strategy to constrain the density parameters associated with dark energy and dark matter.

ACKNOWLEDGMENTS

The authors thank CNPq for the grants under which this work was carried out. JSA is also supported by Fundação de Amparo à Pesquisa do Estado do Rio de Janeiro (FAPERJ). The authors are also grateful to A.F.F. Teixeira for valuable discussions.

REFERENCES

- Alcaniz J.S., 2004, Phys. Rev. D69, 083521. astro-ph/0312424.
- Alcaniz J.S. and Pires N., 2004, Phys. Rev. D 70, 047303. astro-ph/0404146.
- Allen S. W., Ettori S. and Fabian A. C., 2002a, MNRAS, 324, 877.
- Allen S. W., Schmidt R. W. and Fabian A. C., 2002b, MNRAS, 334, L11.
- Allen S.W., Schmidt R.W., Ebeling H., Fabian A.C. and Speybroeck L. van, 2004, Mon. Not. Roy. Astron. Soc. 353, 457. astro-ph/0405340
- Aurich R., Lustig S. and Steiner F., 2005, Class. Quantum Grav. 22, 2061. astro-ph/0412569.
- Aurich R., Lustig S. and Steiner F., 2005, Class. Quantum Grav. 22, 3443. astro-ph/0504656.
- Bennett C.L. et al., 2003, ApJ 148, 1.
- Bernshtain I.N. and Shvartsman V.F., 1980, Sov. Phys. JETP 52, 814.

6 Rebouças and Alcaniz

Bialek J. J., Evrard A. E. and Mohr J. J., 2001, *Astrophys. J.*, 555, 597.

Bond J.R., Pogosyan D. and Souradeep T., 2000, *Phys. Rev. D* 62, 043005.

Calvão M.O., Gomero G.I., Mota B and Rebouças M.J., 2005, *Class. Quant. Grav.* 22, 1991.

Chen G. and Ratra B., 2004, *Astrophys. J.* 612, L1.

Choudhury T.R. and Padmanabhan T., 2005, *Astron. Astrophys.* 429, 807.

Copi C.J., Huterer D. and Starkman G.D., *astro-ph/0310511*.

Cornish N.J., Spergel D. and Starkman G., 1998, *Class. Quant. Grav.* 15, 2657.

Cornish N.J., Spergel D.N., Starkman G.D. and Komatsu E., 2004, *Phys. Rev. Lett.* 92, 201302.

de Oliveira-Costa A., Smoot G.F. and Starobinsky A.A., 1996, *ApJ.* 468, 457.

de Oliveira-Costa A., Tegmark M., Zaldarriaga M. and Hamilton A., 2004, *Phys. Rev. D* 69, 063516.

Dineen P., Rocha G. and Coles P., *astro-ph/0404356*.

Donoghue E.P. and Donoghue J.F., *astro-ph/0411237*.

Eke V. R., Navarro J. F. and Frenk C. S., 1998, *Astrophys. J.*, 503, 569.

Ettori S., Tozzi P. and Rosati P., 2003, *Astron. Astrophys.*, 398, 879.

Fagundes H.V. and Gausmann E., 1999, *Phys. Lett. A* 261, 235.

Freedman W.L., et al., 2001, *ApJ* 553, 47.

Fukugita M., Hogan C. J. and Peebles P. J. E., 1998, *Astrophys. J.* 503, 518

Gomero G.I., Rebouças M.J. and Tavakol R., 2001a, *Class. Quantum Grav.* 18, 4461 (2001).

Gomero G.I., Rebouças M.J., and Tavakol R., 2001b, *Class. Quantum Grav.* 18, L145.

Gomero G.I., Teixeira A.F.F., Rebouças M.J. and Bernui A., 2002, *Int. J. Mod. Phys. D* 11, 869.

Gundermann J., *astro-ph/0503014*.

Hajian A. and Souradeep T., 2005, *Mon. Not. Roy. Astron. Soc.* 359, 699.

Hajian A. and Souradeep T., *astro-ph/0301590*.

Hajian A., Souradeep T. and Cornish N., 2005, *ApJ* 618, L63.

Hipolito-Ricaldi W.S. and Gomero G.I., *astro-ph/0507238*.

Lachièze-Rey M. and Luminet J.-P., 1995, *Phys. Rep.* 254, 135.

Lehoucq R., Lachièze-Rey M. and Luminet J.-P., 1996, *Astron. Astrophys.* 313, 339.

Levin J., 2002, *Phys. Rep.* 365, 251.

Levin J., Scannapieco E. and Silk J., 1998, *Class. Quant. Grav.* 15, 2689.

Lima J.A.S., Cunha J.V. and Alcaniz J.S., 2003, *Phys. Rev. D* 68, 023510. *astro-ph/0303388*.

Lima J.A.S., Cunha J.V. and Alcaniz J.S., 2004, *Phys. Rev. D* 69, 083501. *astro-ph/0306319*

Luminet J.-P., Weeks J., Riazuelo A., Lehoucq R., and Uzan J.-P., 2003, *Nature* 425, 593.

Nesseris S. and Perivolaropoulos L., 2004, *Phys. Rev. D* 70, 043531.

Padmanabhan T. and Choudhury T. R., 2003, *Mon. Not. Roy. Astron. Soc.* 344, 823.

Penrose R., *Proc. Cambridge Philos. Soc.* **55**, 137 (1959).

Rebouças M.J., Alcaniz J.S., Mota B. and Makler M., *A&A* (in press). *astro-ph/0511007*.

Rebouças M.J. and Gomero G.I., 2004, *Braz. J. Phys.* 34, 1358.

Riess A.G. et al., 2004, *ApJ* 607, 665

Roos M., *astro-ph/0509089*.

Roukema B.F. and Edge A., 1997, *Mon. Not. R. Astron. Soc.* 292, 105

Roukema B.F. et al., 2004, *Astron. Astrophys.* 423, 821.

Sasaki S., 1996, *PASJ*, 48, L119

Shafieloo A., Alam U., Sahni V. and Starobinsky A.A., *astro-ph/0505329*.

Spergel D.N. et al., 2003, *ApJ Suppl.* 148, 175.

Starkman G.D., 1998, *Class. Quantum Grav.* 15, 2529.

Tegmark M. et al., 2004, *Phys. Rev. D* 69, 103501

Uzan J.-P., Lehoucq R. and Luminet J.-P., 1999, *Astron. Astrophys.* 351, 766.

Weeks J.R., Lehoucq R. and Uzan J.-P., 2003, *Class. Quantum Grav.* 20, 1529.

Weeks J.R., 2003, *Mod. Phys. Lett. A* 18, 2099.

Zhu Z.-H. and Fujimoto M.-K., 2003, *ApJ* 585, 52.